RSC Advances

ROYAL SOCIETY OF CHEMISTRY

www.rsc.org/advances

Journal Name

ARTICLE

Boosting, Probing and Switching-Off Visible Light-Induced Photocurrents in Eumelanin-Porous Silicon Hybrids

Andrea Pinna[a], Fabrizio Simbula[a], Daniela Marongiu[a] Alessandro Pezzella[b], Marco d'Ischia[b] and Guido Mula[*,a]

[a.] *Dipartimento di Fisica, Università degli Studi di Cagliari, Cittadella Universitaria di Monserrato, S.P. 8 km 0.700, I-09042 Monserrato (CA), Italy*
[b.] *Università di Napoli "Federico II", Dipartimento di Scienze Chimiche, Via Cintia 4, I-80126 Napoli, Italy.*

** Corresponding author. Email: guido.mula@unica.it*

Received 00th January 20xx,
Accepted 00th January 20xx

DOI: 10.1039/x0xx00000x

www.rsc.org/

A relatively intense photocurrent density up to 3.8 mA/cm^2 was induced by visible light in n^+-doped porous silicon (*n*-PSi) coated with a eumelanin thin film produced by ammonia-induced solid state polymerization (AISSP) of 5,6-dihydroxyindole (DHI). The photocurrent was not affected by acetic acid vapors but was irreversibly abated by gaseous ammonia. No detectable photocurrent was observed using p^+-PSi as the inorganic substrate. These results point to eumelanin as a powerful enhancer of PSi photoresponse to visible light via hole-type electrical conduction.

Introduction

Excitonic solar cells [1], including chiefly dye-sensitized solar cells (DSSCs)[2,3], provide highly attractive and promising solutions for solar energy conversion. However, despite considerable progress over the past decade, the development of robust and highly efficient photovoltaic devices is still hampered by issues relating to the high costs of silicon-based cells and especially to the slow, trap-limited diffusion processes that mediate electron transport[4], which markedly limit device efficiency at longer visible-light wavelengths. On the other hand, whereas organic materials offer significant advantages in terms of costs, flexibility and processability[5], and environmental impact[6], they usually show lower light absorption coefficients and worse electronic performances[7] compared to inorganic materials. Thus, there is at present growing interest in the design of hybrid organic-inorganic architectures for solar conversion based on a) the rational molecular tailoring of the organic components[8,9], b) efficient control over supramolecular morphology[10], c) suitably designed nanostructured architectures optimizing interactions of the organic and inorganic components to overcome limiting transport mechanisms[11,12].

In the currently expanding frame of Nature-inspired approaches to innovative technological solutions, considerable attention has been directed in recent years to the development of sustainable strategies for eumelanin-improved devices, from photovoltaics [13] to bioelectronics [14] based on the electrical properties of synthetic mimics of eumelanins[15,16]. Eumelanins are the black-to-brown photoprotective pigments of the skin, hair and eyes which derive biogenetically from tyrosine via the oxidative polymerization of 5,6-dihydroxyindole (DHI) and related metabolites[17]. A schematic of the eumelanin synthetic pathway is shown on Scheme 1.

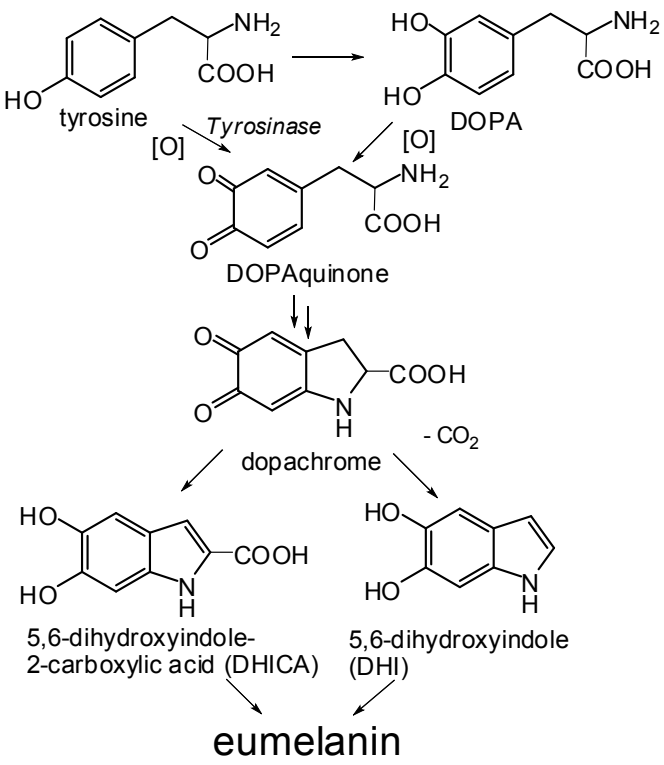

Scheme 1. Overview of the eumelanin synthetic pathway.

Eumelanin-based materials, including DHI polymers and polydopamine, are soft, biocompatible and exhibit a multifunctional and functionalizable heteroaromatic platform combining broadband visible light absorption, a water-dependent hybrid ionic-electronic semiconductor behavior, a distinct free radical character and a peculiar redox reactivity based on catechol/semiquinone/quinone conversion equilibria in the solid state and on the aggregate surface [10,18-20]. Despite persisting issues relating to the structural heterogeneity and poor processability of eumelanins which have limited exploitation in bioinspired photovoltaics, significant advancements are expected from recent reports disclosing expedient approaches for realizing device quality films, such as the ammonia-induced solid state polymerization (AISSP) methodology leading to eumelanin film formation by exposure of DHI thin films to gaseous ammonia.[21]

An attractive inorganic substrate for the development of innovative eumelanin-based hybrids is porous silicon (PSi). PSi has a wide range of biomedical applications[22], from biosensors[23-25] to drug delivery[26-29] and optoelectronics[30-33], and has been used as an antireflection coating for crystalline Si[34-38]. However, very few studies have dealt with its photovoltaic properties [39-41], since most silicon-based organic hybrids thus far considered [43] were constructed on amorphous [44] or crystalline [45] Si. The use of PSi for the realization of plasmonic solar cells has also been explored[46]. Recently[47], we demonstrated that PSi impregnated with synthetic DHI eumelanin exhibits a photoresponse at $\lambda > 500$ nm of potential relevance for solar cells, although the measured photocurrent densities were relatively low (ca. 5 $\mu A/cm^2$). Herein, we report the synthesis of PSi-based hybrids via application of the AISSP methodology for eumelanin film formation[21] which allowed to increase visible light-induced photocurrent densities by more than two orders of magnitude (up to 3.8 mA/cm^2). We show moreover the irreversible inhibition of photocurrent generation following exposure of the hybrid to ammonia vapors. Overall, these results support the relevant technological potential of the AISSP methodology for the development of more efficient PSi-eumelanin hybrids for photovoltaic applications, and yield new important insights into the nature of the elusive photocarriers.

Experimental

Porous silicon

PSi samples were prepared electrochemically from (100)-oriented bulk n^+- and p^+-doped Si wafers. The phosphorous-doped n^+ wafers were from Siltronics and the boron-doped p^+ wafers from Siltronix. The resistivity of both p^+- and n^+-type wafers was in the 0.007-0.003 Ohm/cm range. The detailed procedure for the fabrication of n^+- and a schematic of the cell used is described elsewhere [48]. p^+-PSi was obtained using the same procedure used for n^+-PSi with a HF:H_2O:Ethanol solution in the 35:35:30 percent, respectively. The constant current etching process [48] for both substrates has been performed in a PVC electrochemical cell using the same current (applied for 25s for *n*-PSi and 30s for *p*-PSi samples) for all samples. The silicon substrate acts as the working electrode and a platinum grid is used as a counter electrode. The potential source was a PARSTAT 2273 potentiostat from Princeton Applied Research.

All samples considered have a nominal 1.3μm thickness. The samples' porosity, measured by gravimetry, was 55% (empty/full ratio) for all samples. The external surface of the porosified region is 0.95 cm^2 for all samples.

The optical reflectivity measurements were performed using a PerkinElmer Lambda 950 spectrometer equipped with the Universal Reflectance Accessory using an incidence angle of 8°. We measured absolute reflectivity, that is the reflectivity measured as a percent of the impinging wavelength-dependent light intensity.

Surface morphology was analyzed by atomic force microscopy (AFM) with a NT-MDT Solver P47H-Pro in semicontact mode by a sharp non-contact monocrystal silicon tip.

Eumelanin

Eumelanin polymers for PSi hybrids were prepared from DHI [49] by the previously reported AISSP procedure[21]. The DHI impregnation and the AISSP procedure have been realized within one hour after the porosification of the samples. No intentional modification of the inner pores surface has been done.

Eumelanin immobilization on PSi was obtained treating the substrates with a solution of 2mg DHI in 0.25mL EtOH. The solution was distributed onto the PSi surface by spin coating. The samples were then exposed to gaseous NH_3 for the oxidation and polymerization of DHI. The NH_3 treatment duration was varied during this study to test the procedure, and the standard treatment time was 10'.

Photocurrent measuring procedure

Electrical contacts were realized by deposition of a semitransparent gold contact on top of the empty and impregnated porous layers by sputtering, using an Emitech K450 sputter coater, or by evaporation. The surface of the semitransparent gold contact is 0.64 cm^2. A silver paint drop was then deposited on the deoxidized bulk Si and on the gold film for the measurement. A scheme of a sample ready for the photocurrent measurements is shown in Figure 1.

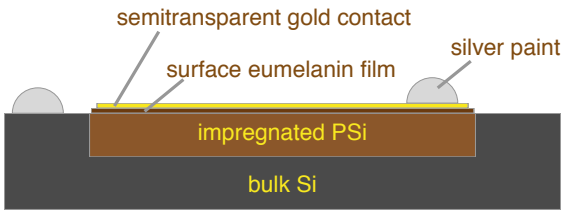

Figure 1: Schematic picture of the eumelanin-impregnated PSi sample employed for the photocurrent measurements.

The samples photoconductivity was tested using a PM8 Analytical prober and a Keithley 2640 multimeter. The light source was a tungsten halogen lamp, whose spectral range at the output of the optical system was in the 400 – 850 nm interval. The illuminated area is about 0.2 cm^2.

Results and Discussion

In the preceding paper [47], photocurrent densities in the order of 5 μA/cm^2 were measured upon exposure to visible light of a PSi-eumelanin hybrid obtained by oxidizing DHI (50 mmol) in phosphate buffer, 0.1 M, pH 7.4, with tyrosinase under a stream of oxygen. Immobilization on PSi was obtained by treating the substrate with the appropriate solution/suspension of DHI or synthetic melanin in methanol, methanol/water, or methanol/phosphate buffer pH 7.0 as the media. When appropriate, tyrosinase was also added to the mixture to promote oxidation process.

In this study, eumelanin film synthesis was carried out with the recently developed AISSP methodology which circumvents issues relating to eumelanin insolubility by allowing in-situ deposition on the inorganic substrate of dark smooth DHI melanin films with improved structural [21].

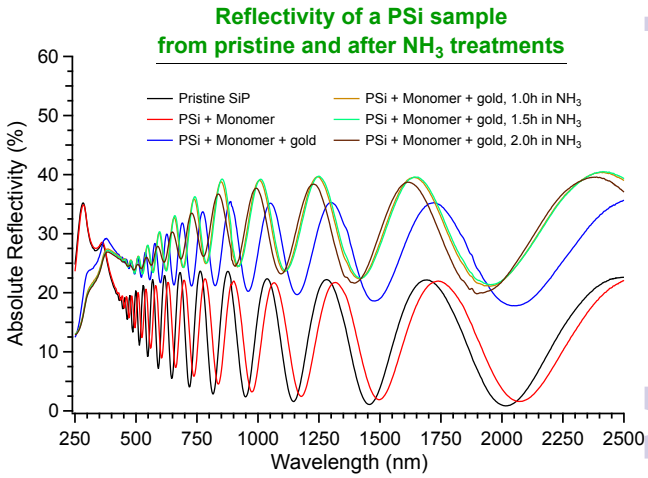

Figure 2. Evolution of the absolute reflectivity of the PSi layers after several treatmer from pristine. The permeability of the gold layer allows for the AISSP treatment of the monomer after the deposition of the surface contact.

The optical properties of the hybrids were investigated by optical reflectivity measurements performed on both untreated and impregnated PSi matrices (a detailed description of the technique and the spectra has been given previously [47]).

Figure 2 reports optical reflectivity spectra of the step-by-step modifications induced in a typical pristine PSi sample by DHI coating, deposition of the gold contacts and AISSP at different times of exposure. The PSi spectrum (black line) is modified by the insertion of the monomer as is shown by the displacement of the interference fringes (red line). Inspection of the modified spectrum ruled out the possible presence of double layers due to limited penetration of eumelanin within the pores, while the displacement demonstrated modification of the average refractive index of the porous layer. This effect is due to the very small pore size (a few tens of nm) with respect to the impinging light wavelength, whereby the light sees the layer as a homogeneous medium with a refractive index resulting from a combination of that of the crystalline skeleton of Si within the PSi layer and that of the air that penetrates the pores. After impregnation of the layer with DHI, the polymer replaces the air within the pores and the average refractive index changes. This does not affect the part of the spectrum (λ < 450nm) relating to bulk Si features. The deposition of the semitransparent gold contact (blue line), with gold reflecting much more than the PSi layer, increases the average reflectivity and, since it cover the PSi layer, reduces the fringes contrast and the shorter wavelengths peaks. It should be noted that the position of the interference fringes remains unchanged, since there is no modification of the porous layer. When the sample is exposed to ammonia (orange, green and brown lines), the fringes are again displaced, their contrast is reduced and there is a further modification of the spectrum for the shorter wavelengths.

The three spectra are quite close, indicating that the modification is mainly achieved by the first treatment with ammonia. Fringes displacement demonstrates that, as in the case of the DHI impregnation, there is a modification of the average refractive index of the porous layer that, in this case, can be easily attributed to a modification of the pores content, due to conversion of DHI to eumelanin. The Si-related features are also modified by the presence of the eumelanin, much stronger absorber that DHI.

The increased reduction of the fringes contrast when moving towards shorter wavelengths is also a good indication that the absorption coefficient of the porous layer is increased, reducing then the interference effect. This is analogous to that already observed in [47] for PSi and PSi with eumelanin.

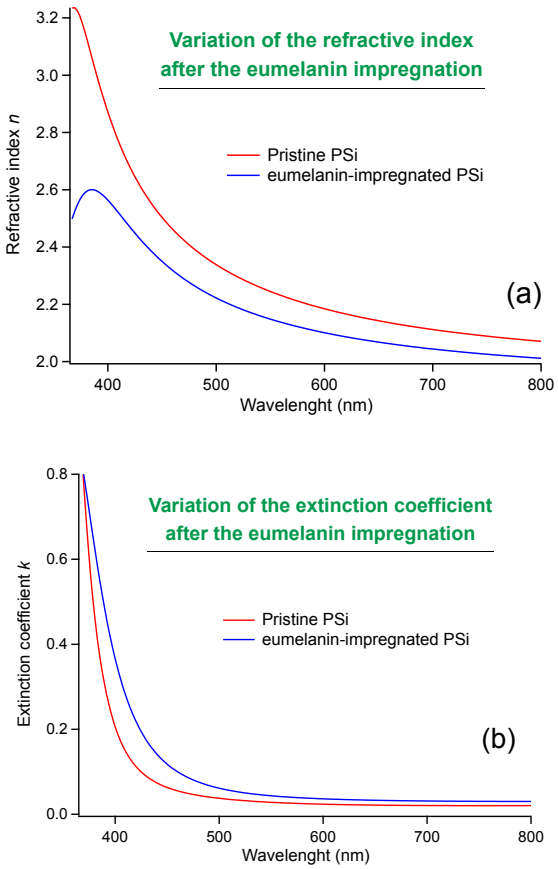

Figure 3. Simulation of the reflectivity spectra of a typical PSi sample before (red line) and after (blue line) the eumelanin impregnation: (a) real part of the complex refractive index (b) extinction coefficient.

The reflectivity spectra of pristine and eumelanin-impregnated PSi samples have been simulated using the SCOUT software from W. Theiss Hard- and Software, Aachen, Germany. In Figure 3 we report the variation of the complex refractive index $n^* = n + ik$ with and without eumelanin obtained by the simulation of the spectra measured in a typical PSi sample used in our study. Figure 3 (a) reports the variation of the real part n and Figure 3 (b) the variation of the extinction coefficient k. While the real part n decreases by a few percent for wavelengths longer than 400 nm after the immobilization, the imaginary part k increases by a maximum of 50%, indicating an increased absorption of the porous layer induced by the presence of the eumelanin.

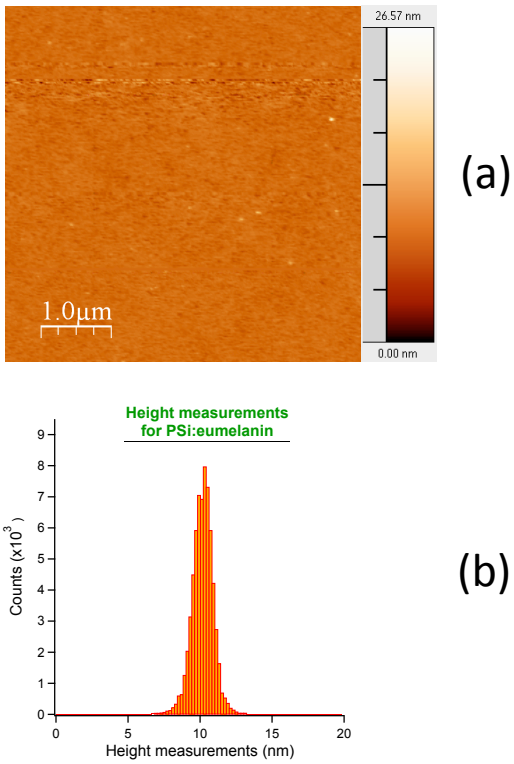

Figure 4. AFM measurements. (a) AFM image of a eumelanin impregnated PSi sample. (b) Histogram of the roughness for the image in (a). The AFM data were elaborated using the WSxM software [50].

The surface morphology of the eumelanin films produced by the AISSP technique were next investigated by AFM. The results indicated an extremely low roughness of the surface of the PSi sample (5-8nm RMS on an average sample) both before and after conversion of the DHI coating by the AISSP technique. The results reported in Figure 4 show an image of an impregnated PSi sample after the AISSP procedure (left) and the corresponding histogram of the surface roughness (right). It is interesting to note that further deposition of eumelanin by a second cycle of DHI coating and AISSP resulted in a significant increase of sample roughness (about 200nm RMS).

Figure 5 shows photocurrents induced in DHI-coated PSi prior to and after AISSP, as a function of cutoff filter wavelength. While simple coating with DHI did not affect the photoelectrical behavior of PSi, the AISSP treatment induced a marked change in the hybrid properties, as evidenced by the higher normalized photocurrent generated by light in the 500-800 nm range compared to untreated sample. Especially worthy of note is the different behavior at $\lambda > 700$ nm: while the DHI-impregnated and pristine PSi samples do not produce significant photocurrent, after the AISSP treatment on the DHI film this low energy spectral region contributes significantly to the total photocurrent, due to black eumelanin synthesis.

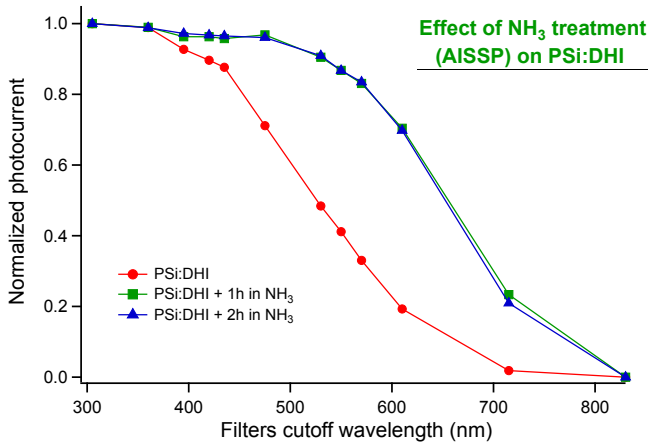

Figure 5 - Normalized photocurrent in DHI-impregnated PSi as a function of cut-off wavelength. Circles refer to measurements before the NH_3 treatment, squares and triangles to measurements after 1 and 2 hours in NH_3 atmosphere, respectively.

Notably, the photocurrent densities recorded in the eumelanin-impregnated hybrid proved to be much higher than those recorded in PSi alone: whereas in the former case a maximum current density of about 3.8 mA/cm^2 was measured, in the latter the maximum current density obtained is 200 µA/cm^2. The measured Open Circuit Potential is about 100mV. A reference test with ammonia-treated pristine PSi showed the same behaviour as untreated pristine PSi. Analysis of I-V plots showed a substantially ohmic behavior up to 1 V, with no detectable voltage in the absence of light. As an additional remark, it is worth noting that no photocurrent was determined on hybrids obtained under the same conditions but using *p*-PSi as the substrate. To gain more insight into the mechanism of photoconduction, in subsequent experiments the effects of acids, water and ammonia on photocurrent intensity and behavior in eumelanin-PSi hybrids were investigated.

The samples were kept in acetic acid or ammonia atmosphere for several time intervals (1-2 h), while water-treated samples were left with a water drop on top of the porous region or left underwater in a crystallizer. The results are shown in Figure 5. In the figure, the PSi 1 ÷ PSi 8 samples names are a reference for the different samples modification through the experimental procedures. All pristine PSi samples are nominally identical.

Figure 6 (a), related to acetic acid treatment, shows that the spectral behaviour of the diffused heterojunction is perfectly maintained after the treatment. The measured white light photocurrent intensity was reduced by a few percent more that the average reduction observed for samples left in air for similar time intervals. Figure 6 (b), related to NH_3 treatment, shows that if the samples, after AISSP, are again exposed to ammonia, this strongly degrades the spectral behaviour of the junction: in addition to the strong reduction of the absolute photocurrent value (over 90% with respect to the same sample before exposure in all cases), the spectral behaviour becomes quite similar to that of pristine PSi samples or samples with monomer DHI. In Figure 6 (c) we observe that the presence of water does not affect the eumelanin signature even though some noise is detected, due probably to measurements unde the water layer. The decrease in the photocurrent was slightly larger than that observed in the samples kept in air.

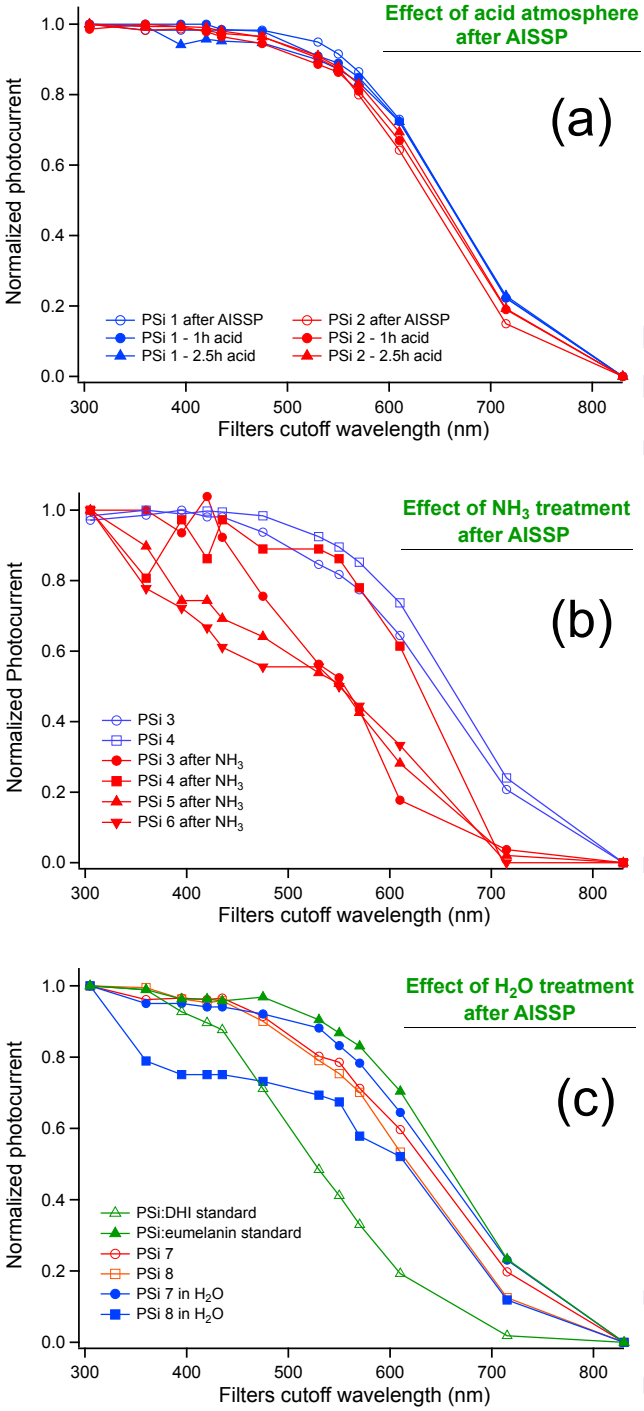

Figure 6. Effects of acetic acid (a), ammonia (b) and water (c) on visible light-induced photocurrents in eumelanin-PSi hybrids.

Thus, these results show that while acetic acid and water do not affect the spectral behaviour of the hybrid, quite unexpectedly a second exposure to ammonia caused a marked decay in the melanin signature photocurrent, gradually

approaching that of pristine PSi. This observation would suggest a depleting effect on the photocarriers. Attempts to restore photocurrents of ammonia-treated samples by subsequent exposure to acids proved unsuccessful, indicating that the effect is virtually irreversible.

Overall, these results provide an unprecedented insight into the nature of the photocarriers involved in the eumelanin-PSi hybrid. Recent studies[20] showed that eumelanin electrical properties can be defined by a water-dependent electronic-ionic hybrid conductor model. In this model, hydration of melanin would shift the comproportionation equilibrium between semiquinones and hydroxyquinone plus quinone species, so as to dope electrons and protons into the system as active charge carriers. This would explain why eumelanin at neutral pH only conducts when "wet". More recently, the mechanism of charge transport in synthetic eumelanin was re-examined and a dominant contribution of ionic processes was demonstrated[18]. In the present study, two observations yield important insights into the nature of the charge carriers involved in the photoelectrical response of eumelanin-PSi hybrids with visible light. First, the requirement for *n*-type doping of PSi in order to have detectable photocurrents with eumelanin would support a prevalent hole-type photoconduction behaviour of eumelanin. Second, the blocking effect of gaseous ammonia would be consistent with an important role of protons as photocarriers, although in this latter case the failure of acetic acid to restore the photocurrent following exposure to ammonia would suggest that other eumelanin-related species might be implicated in hole-type photoconduction, e.g. electrophilic quinonoid units quenchable by covalent interaction with ammonia. In other words, though the effect of ammonia would in principle suggest a proton-based conduction mechanism, the marked difference from a typical proton-based behavior, e.g. reversibility and short current life-times due to ion accumulation on the electrode surface[20,21], would actually support in the present case a complex interplay of carriers and processes which are controlled by proton availability/mobility but are not exclusively ionic in character.

Both observations are of considerable scientific and practical relevance, and deserve further investigations. Based on these lines of evidence, it could be argued that irradiation of the eumelanin component with visible light causes transition of the surface components of the polymer to the excited state. This latter state would then evolve through non-radiative deactivation channels involving, e.g. electron transfer to molecular oxygen, with generation of oxidized species such as radical cations and quinones, and excited state proton transfer (ESPT)[51,52] (Scheme 2).

Thus, both photooxidation and ESPT processes may overall concur to the onset of photocurrents via radical cation generation and efficient sequential transfer of protons from highly acidic excited states to the surrounding acceptor functionalities, including basic indole rings and phenolic groups.

Investigation of ionic conductivity data of DHI melanin-coated PSi films following treatment with acids, ammonia or wate will provide a tool for further more quantitative insight into the important issue of melanin conductivity mechanisms.

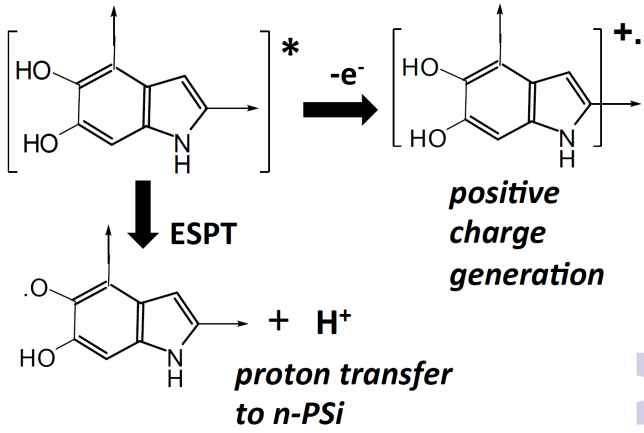

Scheme 2 - Schematic representation of charge carrier generation by irradiation of eumelanin layer on PSi. Dual concurrent pathways of excited state deactivation are highlighted: 1) electron transfer to molecular oxygen, leading to the generation of radical cation species from DHI units; 2) excited state proton transfer (ESPT) to adjacent eumelanin components and/or to *n*-PSi.

Conclusions

In this study we report an improved solid state polymerization methodology for eumelanin film deposition on *n*-doped PSi which resulted in a two orders of magnitude increase in visible light-induced photocurrents compared to previously used technology based on deposition of preformed eumelanin polymers. Most interestingly, an irreversible drop in photocurrent was caused by exposure to ammonia vapours, whereas acetic acid vapours did not affect the electrical properties of the hybrid. These results: a) contribute to expand the scope of bulk diffuse heterojunctions for optoelectronic applications; b) provide evidence for the light harvesting capability of eumelanin, serving as an antenna in hybrid devices; c) yield new insights into the mechanisms of photoconduction of eumelanin films.

These results open the doorway to various possible applications of eumelanin-porous silicon hybrids, e.g. for solar cells, photodetection or biosensing. However, while photocurrent data are reasonable, some important interface issues still need to be settled before specific devices based on the reported hybrid can be devised and engineered. The optimization of the interface is a key goal of ongoing studies, which will be specifically directed to assess relevant issues such as the dependence of the photocurrent on thickness of the eumelanin layer and the role of pore size and porosity.

Acknowledgements

This work was supported in part by Italian MIUR, PRIN 2010-2011 PROxi project.

References

1 B.A. Gregg, *J. Phys. Chem. B*, 2003, **107** (20), 4688.
2 M. Grätzel, *J. Photoch. Photobio. C*, 2003, **4**, 145
3 Md. K. Nazeeruddin, E. Baranoff, M. Grätzel, *Sol. Energy*, 2011, **85**, 1172.
4 M. Law, L.E. Greene, J.C. Johnson, R. Saykally, P. Yang, *Nat. Mater.,* 2005, **4**, 455.
5 W. Cai, X. Gong, Y. Cao, *Sol. Energ. Mat. Sol. C.*, 2010, **94**, 114.
6 Y.-S. Zimmermann, A. Schäffer, C. Hugi, Karl Fent, Philippe F.-X. Corvini, Markus Lenz, *Environ. Int.*, 2012, **49**, 128.
7 L. Reijnders, *J. Clean. Prod.*, 2010, **18**, 307.
8 L. Tsakalakos, *Nanotechnology for photovoltaics*, CRC Press, Taylor & Francis Group, Boca Raton, FL, USA (2010)
9 U. Wiesner, *Hybrid Polymer–Inorganic Nanostructures, in Polymer Science: A Comprehensive Reference*, Eds. Krzysztof Matyjaszewski and Martin Möller, Vol. 7: *Nanostructured Polymer Materials and Thin Films*, 2012, 129–140, Elsevier B.V, Amsterdam, The Netherlands, 2012
10 P. Meredith and T. Sarna, *Pigm. Cell Res.*, 2006, **19**, 572.
11 B.A. Stickler, M. Gruber, G. Trimmel, F. Schürrer, K. Zojer Org. Electron., 2011, **12**, 1434.
12 M. Gruber, B.A. Stickler, G. Trimmel, F. Schürrer, K. Zojer, *Org. Electron.,* 2010, **11**, 1999.
13 V. Capozzi, G. Perna, P. Carmone, A. Gallone, M. Lastella, E. Mezzenga, G. Quartucci, M. Ambrico, V. Augelli, P.F. Biagi, T. Ligonzo, A. Minafra, L. Schiavulli, M. Pallara, R. Cicero, *Thin Sol. Films*, 2006, **511–512**, 362.
14 M. Ambrico, P.F. Ambrico, T. Ligonzo, A. Cardone, S.R. Cicco, M. d'Ischia, G.M. Farinola, *J. Mat. Chem. C*, 2015, Ahead of Print.
15 M. d'Ischia, A. Napolitano, V. Ball, C.-T. Chen, M.J. Buehler, *Acc. Chem. Res*. 2014, **47**, 3541.
16 L. Morresi, M. Ficcadenti, N. Pinto, R. Murri, M. Cuccioloni, M. Angeletti, P. Tombesi, *Energy Procedia*, 2010, **2**, 177.
17 S. Ito, K. Wakamatsu, M. d'Ischia, A. Napolitano, A. Pezzella, in *Melanins and Melanosomes: Biosynthesis, Biogenesis, Physiological, and Pathological Functions* Eds: P.A. Riley, J. Borovansky, Wiley-VCH , Germany, Ch. 6, 167 – 185.
18 J. Wünsche, Y. Deng, P. Kumar, E. Di Mauro, E. Josberger, J. Sayago, A. Pezzella, F. Soavi, F. Cicoira, M. Rolandi, C. Santato, *Chem. Mater.*, 2015, **27**, 436.
19 G. Tarabella, A. Pezzella, A. Romeo, P. D'Angelo, N. Coppedè, M. Calicchio, M. d'Ischia, R. Mosca, S. Iannotta, *J. Mater. Chem. B*, 2013, **1**, 3843.
20 A.B. Mostert, B.J. Powell, F.L. Pratt, G.R. Hanson, T, Sarna, I.R. Gentle, P. Meredith, *Proc. Natl. Acad. Sci. USA*, 2012, **109**, 8943.
21 A. Pezzella, M. Barra, A. Musto, A. Navarra, M. Alfe, P. Manini, S. Parisi, A. Cassinese, V. Criscuolo, M. d'Ischia, *Mater. Horizons* 2015, **2,** 212.
22 Porous silicon for biomedical applications, Ed. Hélder A. Santos, Woodhead Publishing, Sawston, Cambridge, UK, 2014
23 S. Dhanekar, S. Jain, *Biosens. Bioelectron.*, 2013, **41**, 54.
24 C. RoyChaudhuri, *Sensors Actuat. B: Chem.*, 2015, **210**, 310.
25 F.A. Harraz, *Sensors Actuat. B: Chem.*, 2014, **202**, 897.
26 E.J. Anglin, L. Cheng, W.R. Freeman, M.J. Sailor, *Adv. Drug Deliver. Rev.*, 2008, **60**, 1266.
27 K.L. Jarvis, T.J. Barnes, C.A. Prestidge*, Adv. Colloid Interf.*, 2012, **175**, 25.
28 J. Hernandez-Montelongo, N. Naveas, S. Degoutin, N. Tabary, F. Chai, V. Spampinato, G. Ceccone, F. Rossi, V. Torres-Costa, M. Manso-Silvan, B. Martel, Carbohyd. Polym., 2014, **110**, 238.
29 M.A. Tölli, M.P.A. Ferreira, S.M. Kinnunen, J. Rysä, E.M. Mäkilä, Z. Szabó, R.E. Serpi, P.J. Ohukainen, M.J. Välimäki, A.M.R. Correia, J.J. Salonen, J.T. Hirvonen, H.J. Ruskoaho, H.A. Santos, *Biomaterials*, 2014, **35**, 8394.
30 O. Bisi, S. Ossicini, L. Pavesi, *Surf. Sci. Rep.*, 2000, **38**, 1.
31 A.J Kenyon, *Prog. Quant. Electron.*, 2002, **26**, 225.
32 A.B. Djurišic´, A.M.C. Ng, X.Y. Chen, *Prog. Quant. Electron.*, 2010, **34,** 191.
33 M.B. de la Mora, C. Torres-Torres, R. Nava, M. Trejo-Valdez, J.A. Reyes-Esqueda, *Opt. Laser Technol.*, 2014, **59**, 104.
34 W.J. Aziz, A. Ramizy, K. Ibrahim, Z. Hassan, K. Omar, *Optik – Intl. J. Light Electron Opt.,* 2011, **122**, 1462.
35 J.H. Selj, E.S. Marstein, A. Thøgersen, S.E. Foss, *Phys. Stat. Sol. C*, 2011, **8**, 1860.
36 K.A. Salman, K. Omar, Z. Hassan, *Superlattice. Microst.*, 2011, **50**, 647.
37 T.D. Dzhafarov, S.S. Aslanov, S.H. Ragimov, M.S. Sadigov, S. Aydin Yuksel, *Vacuum*, 2012, **86**, 1875.
38 W.A. Badawy, *J. Adv. Res.*, 2015, **6**, 123.
39 B. Ünal, A.N. Parbukov, S.C. Bayliss, *Opt. Mater.*, 2001, **17**, 79.
40 V. Capozzi, G. Perna, P. Carmone, A. Gallone, M. Lastella, Mezzenga, G. Quartucci, M. Ambrico, V. Augelli, P.F. Biagi, T. Ligonzo, A. Minafra, L. Schiavulli, M. Pallara, R. Cicero, *Th… Sol. Films* 2006, **511-512**, 362.
41 A. Nahor, O. Berger, Y. Bardavid, G. Toker, Y. Tamar, L. Reis… M. Asscher, S. Yitzchaik, A. Sa'ar, *Phys. Stat. Sol. C*, 2011, **8**, 1908.
42 A. Nahor, I. Shalev, A. Sa'ar, S. Yitzchaik, Eur. J. Inorg. Chem., 2015, **2015**, 1212.
43 T. Mayer, U. Weiler, C. Kelting, D. Schlettwein, S. Makarov, D. Wöhrle, O. Abdallah, M. Kunst, W. Jaegermann, *Sol. Energ. Mat. Sol. C.*, 2007, **91**, 1873.
44 C.-H. Chao, C.-H. Chan, F.-C. Wu, J.-J. Huang, S.Y. Lien, K.-W. Weng, H.-L. Cheng. *Sol. Energ. Mat. Sol. C.*, 2011, **95**, 2407.
45 V.P. Zubov, A.A. Ishchenko, P.A. Storozhenko, I.V. Bakeeva, Yu.O. Kirilina, G.V. Fetisov, *Dokl. Chem*. 2011, **437**, 120.
46 S. Sánchez de la Morena, G. Recio-Sánchez, V. Torres-Costa, R.J. Martín-Palma, *Scripta Mater.,* 2014, **74**, 33.
47 G. Mula, L. Manca, S. Setzu, A. Pezzella, *Nanosc. Res. Lett.* 2012, **7**, 377.
48 G. Mula, S. Setzu, G. Manunza, R. Ruffilli, A. Falqui, *J. Phys. Chem. C*, 2012, **116**, 11256.
49 R. Edge, M. d'Ischia, E. J. Land, A. Napolitano, S. Navaratnam, L. Panzella, A. Pezzella, C. A. Ramsden, P. A. Riley, Pigm. *Cell Res.,* 2006, **19**, 443.
50 I. Horcas, R. Fernandez, J.M. Gomez-Rodriguez, J. Colchero, J. Gomez-Herrero and A. M. Baro, *Rev. Sci. Instrum*. 2007, **78**, 013705.
51 M. Gauden, A. Pezzella, L. Panzella, A. Napolitano, M. d'Ischia V. Sundström, *J. Phys. Chem. B*, 2009, **113**, 12575.
52 A. Corani, A. Huijser, T. Gustavsson, D. Markovitsi, Per-Åke Malmqvist, A. Pezzella, M. d'Ischia, V. Sundström, *J. Am. Chem. Soc.*, 2014, **136**, 11626.

Graphical abstract

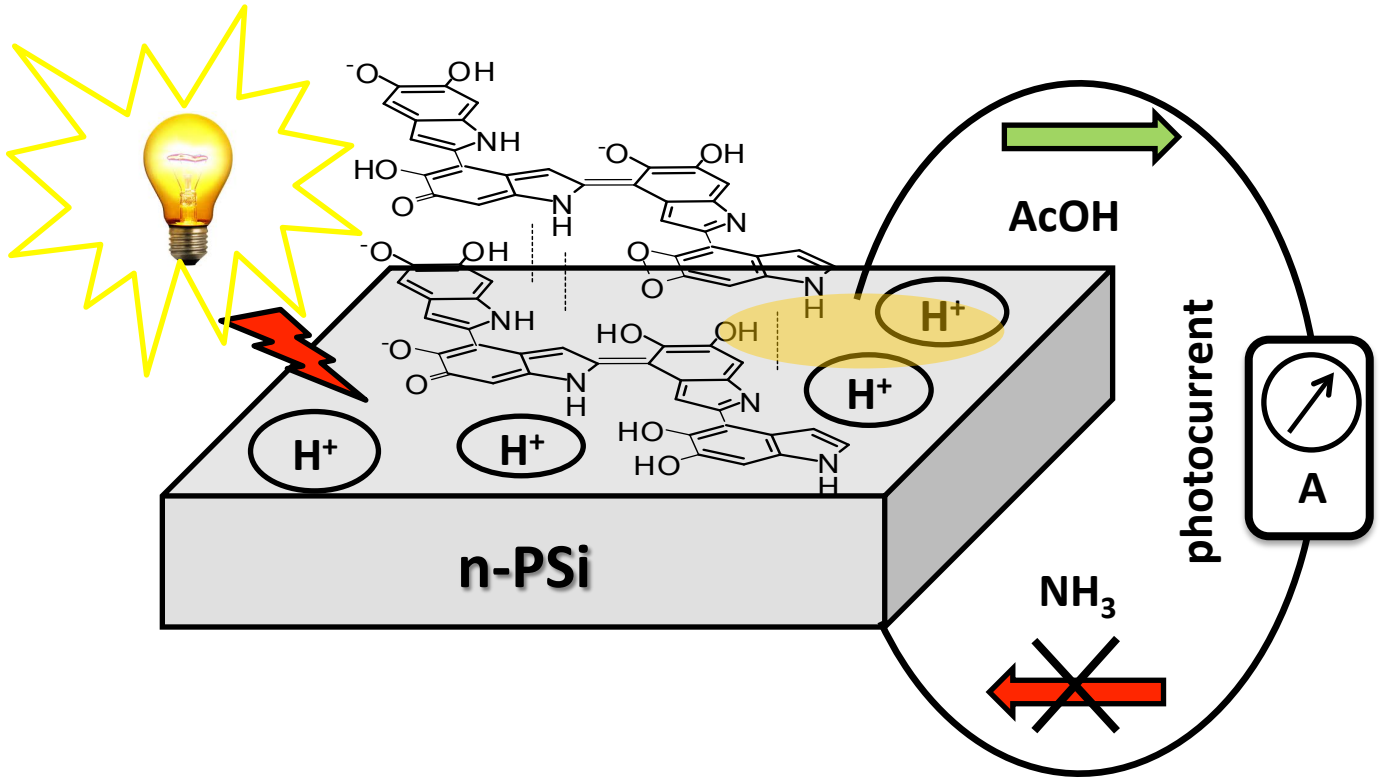

Improved solid state polymerization of eumelanin in porous silicon and new insights into the mechanisms of photoconduction of eumelanin films